

A schematic diagram of a lithium-ion battery. The main part of the image shows a dark green, textured matrix with a complex network of yellow, branching conductive pathways. A circular inset on the right provides a detailed view of a hexagonal pore structure. Inside this pore, a yellow line represents a conductive pathway. A lithium ion (Li^+) is shown moving along this pathway, and an electron (e^-) is shown moving in the opposite direction.

GDCh

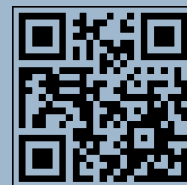
GESELLSCHAFT
DEUTSCHER CHEMIKER

Get the **Angewandte App**
International Edition



Enjoy Easy Browsing and a New Reading Experience on Your Smartphone or Tablet

- Keep up to date with the latest articles in Early View.
- Download new weekly issues automatically when they are published.
- Read new or favorite articles anytime, anywhere.



Service

Spotlight on Angewandte's Sister Journals

9464 – 9467

Author Profile



"My favorite food is Sushi.

If I were not a scientist, I would be an architect, artist, or designer of some sort. ..."

This and more about Jón T. Njarðarson can be found on page 9468.

Jón T. Njarðarson _____ 9468

Obituaries



The German-born American historian Fritz Stern passed away on May 18, 2016 in New York. Stern dedicated his life's work to the study of European, particularly German, cultural history. Well aware that Germany's rise to preeminence during the 19th century was rooted in its scientific-technological culture, Fritz Stern created a portrait gallery of key protagonists of that "age of genius" which included Fritz Haber, his godfather.

Fritz Stern (1926–2016)

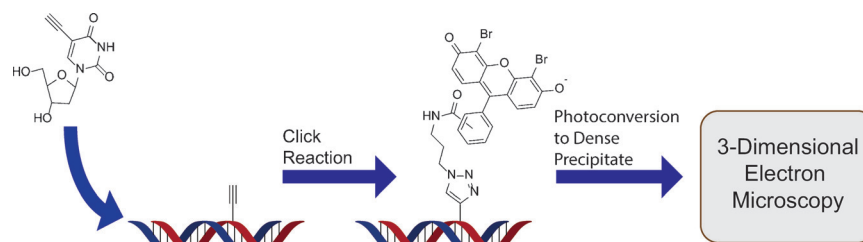
G. Ertl, B. Friedrich* _____ 9470 – 9471

Highlights

Imaging

D. M. van Elsland,
S. I. van Kasteren* — 9472–9473

Imaging Bioorthogonal Groups in Their
Ultrastructural Context with Electron
Microscopy



Spitting image: Herein a recent paper on the imaging of bioorthogonal groups using three-dimensional electron microscopy is discussed. The work has demon-

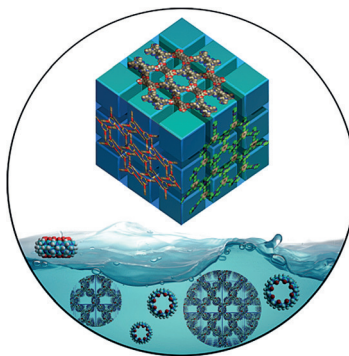
strated electron microscopy imaging as a technique suitable for gaining structural information on bioorthogonal groups in their cellular context.

Minireviews

Supramolecular Chemistry

J. Lü, R. Cao* — 9474–9480

Porous Organic Molecular Frameworks
with Extrinsic Porosity: A Platform for
Carbon Storage and Separation



Porous organic molecular frameworks (POMFs) have recently been discovered as a new class of chemical materials for carbon storage and separation. The assembly of POMFs by means of primary hydrogen bonding interactions is reviewed based on their applications in both the solid state and solution phase.

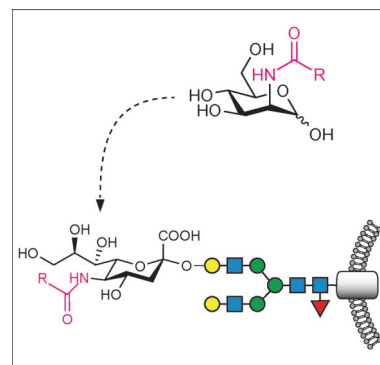
Reviews

Metabolic Glycoengineering

P. R. Wrtil,* R. Horstkorte,*
W. Reutter* — 9482–9512

Metabolic Glycoengineering with *N*-Acyl
Side Chain Modified Mannosamines

Sugar for cells: Metabolic glycoengineering is a method to incorporate modified monosaccharides into cells, organs, or animals. Unnatural sialic acids can be generated by treatment with *N*-acyl side chain modified mannosamines. The application of this technique has intriguing biological consequences for treated cells. Mannosamine analogues bearing reactive groups can be used, for example, to visualize sialylated glycoconjugates.

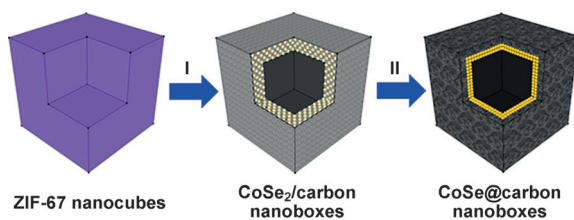


For the USA and Canada:

ANGEWANDTE CHEMIE International Edition (ISSN 1433-7851) is published weekly by Wiley-VCH, PO Box 101161, 69451 Weinheim, Germany. US mailing agent: SPP, PO Box 437, Emigsville, PA 17318. Periodicals postage

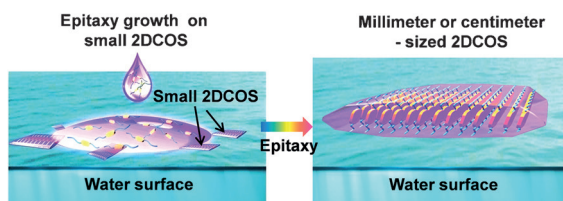
paid at Emigsville, PA. US POSTMASTER: send address changes to *Angewandte Chemie*, John Wiley & Sons Inc., C/O The Sheridan Press, PO Box 465, Hanover, PA 17331. Annual subscription price for institutions: US\$ 16.862/14.051 (valid for print and electronic / print or

electronic delivery); for individuals who are personal members of a national chemical society prices are available on request. Postage and handling charges included. All prices are subject to local VAT/sales tax.



Box clever: Hybrid nanoboxes composed of a CoSe-enriched inner shell confined within a carbon-enriched outer shell are synthesized by a template-based method. With their structural and compositional

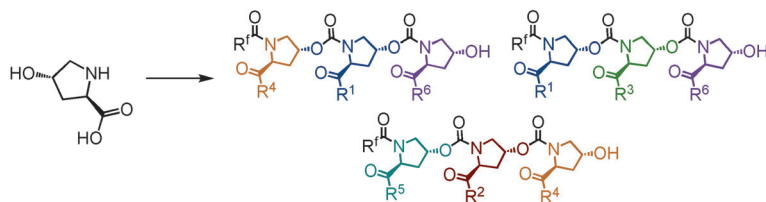
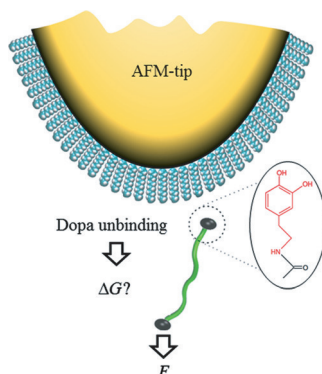
advantages, these unique CoSe@carbon nanoboxes exhibit a superior electrochemical performance as an anode material for lithium-ion batteries.



Water of crystallization: A novel method named "solution epitaxy" for the growth of 2D crystals of organic semiconductors (2DCOS) is based on the self-assembly of

micrometer-sized 2DCOS on a water surface, and then epitaxial growth into centimeter sized 2DCOS with thickness of several molecular layers.

Biophysics: Dopa-surface interactions are very important for nanotechnology and surface modification (Dopa = 3,4-dihydroxyphenylalanine). The binding energies between Dopa and various surfaces were determined by single-molecule force spectroscopy (see picture; ΔG = free energy and F = force).



Another link in the chain: A controlled synthesis of novel oligomers from hydroxyproline-based building blocks was developed. The hydroxyproline-based monomer allows the incorporation of diverse side chains, and high-throughput

purification can be achieved by fluororous solid-phase extraction. This method is adaptable to high-throughput synthesis in multiwell plates, thus allowing hundreds of novel oligomer structures to be synthesized in parallel.

Communications

Hybrid Nanomaterials

H. Hu, J. T. Zhang, B. Y. Guan, X. W. Lou* — 9514–9518

Unusual Formation of CoSe@carbon Nanoboxes, which have an Inhomogeneous Shell, for Efficient Lithium Storage



Frontispiece

Organic Semiconductors

C. Xu, P. He, J. Liu, A. Cui, H. Dong, Y. Zhen, W. Chen, W. Hu* — 9519–9523

A General Method for Growing Two-Dimensional Crystals of Organic Semiconductors by "Solution Epitaxy"



Front Cover

Surface Chemistry

T. Utzig,* P. Stock, M. Valtiner* — 9524–9528

Resolving Non-Specific and Specific Adhesive Interactions of Catechols at Solid/Liquid Interfaces at the Molecular Scale



Biomaterials

R. L. Kanasty, A. J. Vegas, L. M. Ceo, M. Maier, K. Charisse, J. K. Nair, R. Langer, D. G. Anderson* — 9529–9533

Sequence-Defined Oligomers from Hydroxyproline Building Blocks for Parallel Synthesis Applications



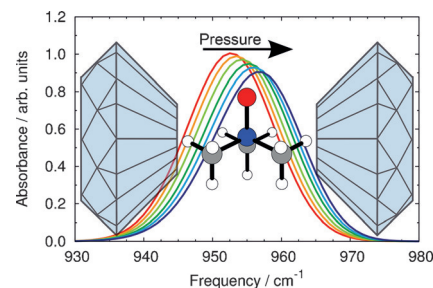
Vibrational Spectroscopy

S. Imoto,* P. Kibies, C. Rosin, R. Winter,*
S. M. Kast, D. Marx — 9534–9538



Toward Extreme Biophysics: Deciphering the Infrared Response of Biomolecular Solutions at High Pressures

Squeeze it out of them: Trimethylamine N-oxide (TMAO) is known to stabilize protein structures at extreme pressures, possibly through hydrogen bonding. A combination of FTIR spectroscopy and computer simulation has now been used to connect pressure-induced changes in the IR spectrum of TMAO (see picture) to a locally enhanced hydrogen-bonding network at high compression. The insight gained should be transferable to biomolecules in their native solvent.



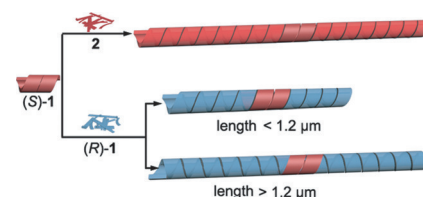
Chiral Nanotubes

X. Ma, Y. Zhang, Y. Zhang, Y. Liu, Y. Che,*
J. Zhao — 9539–9543



Fabrication of Chiral-Selective Nanotubular Heterojunctions through Living Supramolecular Polymerization

A perfect role model: Chiral-selective linear nanotubule heterojunctions were achieved by living self-assembly. Chiral perylene-3,4,9,10-tetracarboxylic diimide (PDI)-based nanotube seed (S)-1 not only induced the supramolecular polymerization of microribbons of an achiral PDI derivative 2 at the seed ends in the same helical sense but could also polymerize the opposite enantiomer (R)-1 in the same helical sense; this biasing depended on the final tube length.



Biophysics

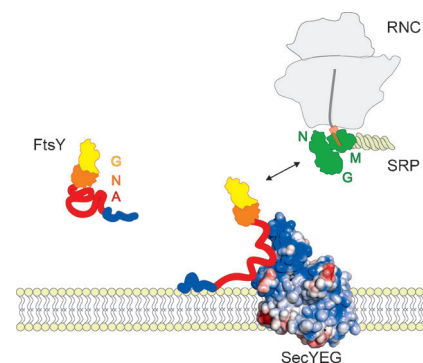


N. A. Lakomek,* A. Draycheva,
T. Bornemann,
W. Wintermeyer* — 9544–9547



Electrostatics and Intrinsic Disorder Drive Translocon Binding of the SRP Receptor FtsY

Integral membrane proteins in bacteria are co-translationally targeted to the translocon for membrane insertion via the signal recognition particle (SRP) pathway. The SRP receptor FtsY and its N-terminal A domain, which is lacking in any structural model of FtsY, were studied using NMR and fluorescence spectroscopy. Translocon targeting and binding of FtsY is driven by electrostatic interactions of the intrinsically disordered A domain.

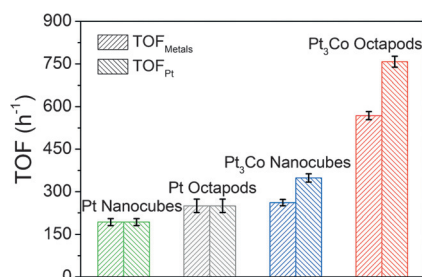


Heterogeneous Hydrogenation

M. U. Khan, L. Wang, Z. Liu, Z. Gao,
S. Wang, H. Li, W. Zhang, M. Wang,
Z. Wang,* C. Ma, J. Zeng* — 9548–9552

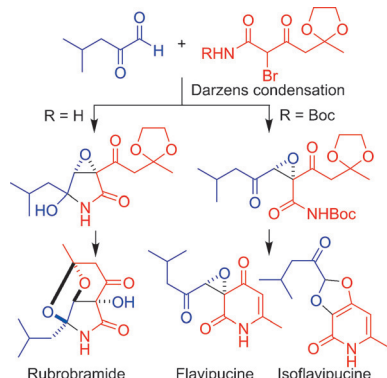


Pt₃Co Octapods as Superior Catalysts of CO₂ Hydrogenation



Pt₃Co octapods, Pt₃Co nanocubes, Pt octapods, and Pt nanocubes were used as catalysts for carbon dioxide hydrogenation. Owing to the multiple sharp tips and the charge transfer between Pt and Co, which leads to the accumulation of negative charge on the Pt atoms in the vertices, the Pt₃Co octapods were the most efficient catalyst of this process.

Inside Cover

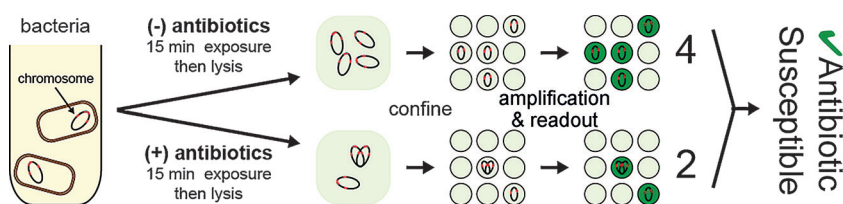


Three pieces: Total synthesis of (\pm)-rubrobramide, (\pm)-flavipucine, and (\pm)-isoflavipucine was achieved by a Darzens reaction between isobutyl glyoxal and α -bromo- β -ketoamides, removal of the protecting group(s), and ring formation. After optical resolution of synthetic (\pm)-rubrobramide, the absolute configuration of naturally occurring (+)-rubrobramide was determined by vibrational circular dichroism.

Natural Products

S. Mizutani, K. Komori, T. Taniguchi, K. Monde, K. Kuramochi,* K. Tsubaki _____ **9553 – 9556**

A Bioinspired Synthesis of (\pm)-Rubrobramide, (\pm)-Flavipucine, and (\pm)-Isoflavipucine



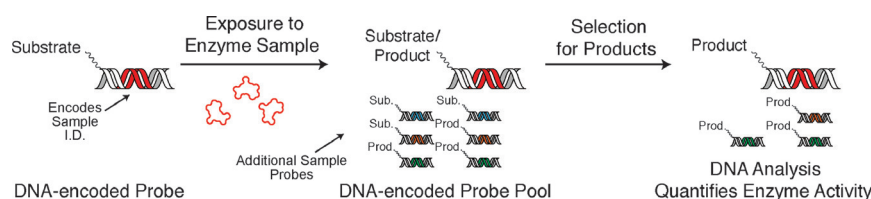
Single-molecule counting was used to detect subtle changes in the amount and the assembly state of bacterial chromosomes after a short exposure of live bacteria to antibiotics. The method

employed digital PCR to determine the susceptibility of *E. coli* clinical isolates from urinary tract infections to four different antibiotics.

Analytical Methods

N. G. Schoepp, E. M. Khorosheva, T. S. Schlappi, M. S. Curtis, R. M. Humphries, J. A. Hindler, R. F. Ismagilov* _____ **9557 – 9561**

Digital Quantification of DNA Replication and Chromosome Segregation Enables Determination of Antimicrobial Susceptibility after only 15 Minutes of Antibiotic Exposure



DNA-linked peptide substrates are used as probes of enzymatic activity. Encoding the sample identity in the DNA enables sensing of activity by DNA analysis. Probe phenotypes can be altered from substrate

to product by enzyme exposure, affecting survival in a downstream selection. Selection-induced changes in probe frequency within a population quantify enzyme activity.

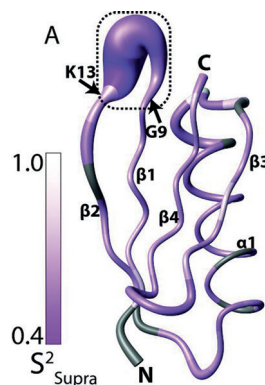
Analytical Methods

R. R. Jetson, C. J. Krusemark* _____ **9562 – 9566**

Sensing Enzymatic Activity by Exposure and Selection of DNA-Encoded Probes



A link is made between ground-state conformational inter-conversion and molecular recognition. High-power relaxation dispersion measurements at super-cooled temperatures, together with an ensemble representation of the third IgG-binding domain of protein G derived from residual dipolar couplings, point to a role for supra- τ_c dynamics in molecular recognition.



Protein Dynamics

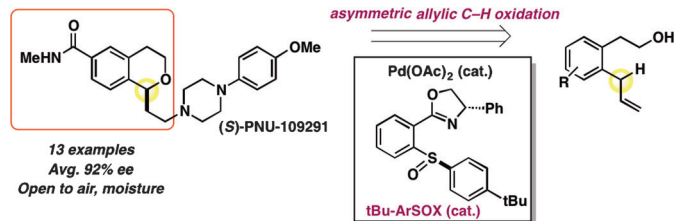
S. Pratihari, T. M. Sabo, D. Ban, R. B. Fenwick, S. Becker, X. Salvatella, C. Griesinger,* D. Lee* _____ **9567 – 9570**

Kinetics of the Antibody Recognition Site in the Third IgG-Binding Domain of Protein G



Asymmetric Catalysis

S. E. Ammann, W. Liu,
M. C. White* 9571–9575



Selective and general: Palladium(II)/chiral sulfoxide catalysis affords an asymmetric allylic C–H oxidation reaction which proceeds with broad scope and high levels of enantioselectivity. The

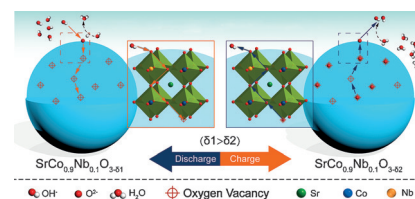
palladium(II)/ArSOX catalyst furnishes chiral isochromans from terminal olefin precursors and the reactions are run open to the air and moisture.

Energy Storage

L. Zhu, Y. Liu, C. Su, W. Zhou, L. M. Liu,*
Z. P. Shao* 9576–9579

Perovskite $\text{SrCo}_{0.9}\text{Nb}_{0.1}\text{O}_{3-\delta}$ as an Anion-Intercalated Electrode Material for Supercapacitors with Ultrahigh Volumetric Energy Density

Supercapacitors: The perovskite $\text{SrCo}_{0.9}\text{Nb}_{0.1}\text{O}_{3-\delta}$ (SCN) is a highly promising electrode material with an ultrahigh volumetric energy density for supercapacitors. Through an anion-insertion mechanism, this nonporous perovskite material cannot only achieve a high capacitance, but also shows an outstanding rate capability and excellent cycling stability.

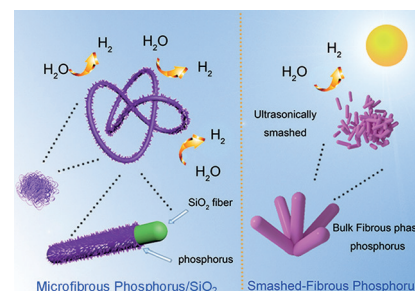


Photocatalysis

Z. H. Hu, L. Y. Yuan, Z. F. Liu, Z. R. Shen,*
J. C. Yu* 9580–9585

An Elemental Phosphorus Photocatalyst with a Record High Hydrogen Evolution Efficiency

A breakthrough: Fibrous-phase red phosphorous was used as semiconductor photocatalyst for visible-light-driven hydrogen evolution. The phosphorus in micro-fibrous P/SiO_2 and smashed-fibrous phosphorus showed hydrogen evolution rates of $633 \mu\text{mol h}^{-1} \text{g}^{-1}$ and $684 \mu\text{mol h}^{-1} \text{g}^{-1}$, respectively. These values are records for elemental photocatalysts.

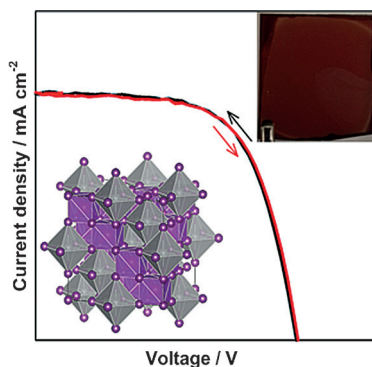


Inside Back Cover

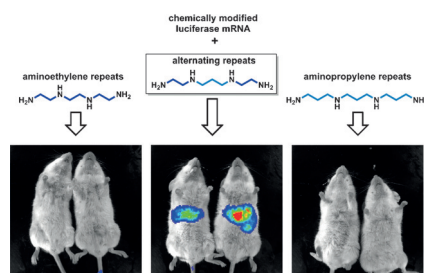
Thin-Film Photovoltaics

Y. Kim, Z. Yang, A. Jain, O. Voznyy,
G.-H. Kim, M. Liu, L. N. Quan,
F. P. García de Arquer, R. Comin, J. Z. Fan,
E. H. Sargent* 9586–9590

Pure Cubic-Phase Hybrid
Iodobismuthates AgBi_2I_7 for Thin-Film
Photovoltaics



Solution-processed AgBi_2I_7 thin films are developed and deployed to produce air-stable and lead-free photovoltaic devices. The AgBi_2I_7 thin film crystallized in the cubic phase with dense and pinhole-free surface morphologies, and has an optical absorption that covers the visible spectrum and into the near-infrared region. The AgBi_2I_7 devices showed stable operation over 10 days under ambient conditions.



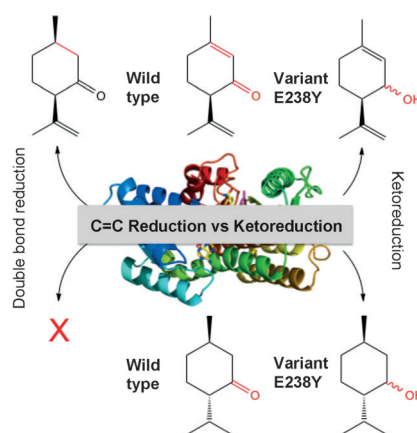
Oligoalkylamine-based lipids and polymers were generated and screened for buffering capacity and mRNA delivery. Alternating ethylene/propylene/ethylene spacers in the tetramines improve transfection efficiency (see picture, middle) over ethylene-only (left) or propylene-only repeats (right). This trend is valid regardless of delivery platform (lipids or polymers), tested cell line, targeted tissue, or application route in vivo.

mRNA Delivery

A. Jarzębińska, T. Pasewald, J. Lambrecht, O. Mykhaylyk, L. Kümmerling, P. Beck, G. Hasenpusch, C. Rudolph, C. Plank, C. Dohmen* **9591 – 9595**

A Single Methylene Group in Oligoalkylamine-Based Cationic Polymers and Lipids Promotes Enhanced mRNA Delivery

A simple mechanistic switch: The replacement of tyrosine by glutamic acid in (–)-menthone:(+)-neomenthol reductase and of glutamic acid by tyrosine in isopiperitenone reductase enabled a switch between ene-reductase and ketoreduction activity in the short-chain dehydrogenases/reductases superfamily. This provides attractive routes to novel ene-reductase catalysts.



Enzyme Modifications

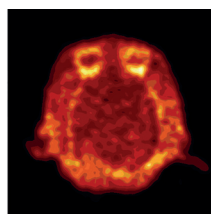
A. Lygidakis, V. Karuppiiah, R. Hoeven, A. Ní Cheallaigh, D. Leys, J. M. Gardiner, H. S. Toogood, N. S. Scrutton* **9596 – 9600**

Pinpointing a Mechanistic Switch Between Ketoreduction and “Ene” Reduction in Short-Chain Dehydrogenases/Reductases



A highly potent inhibitor has been identified as a highly selective antagonist of glycogen synthase kinase-3 (GSK-3). Its efficacy in modulation of tau phosphorylation was demonstrated. A ^{11}C -isotopo-

logue was synthesized, and preliminary PET imaging studies confirmed that the two major obstacles for imaging GSK-3 have been overcome: reasonable brain permeability and displaceable binding.



Phosphorylation

S. H. Liang, J. M. Chen, M. D. Normandin, J. S. Chang, G. C. Chang, C. K. Taylor, P. Trapa, M. S. Plummer, K. S. Para, E. L. Conn, L. Lopresti-Morrow, L. F. Lanyon, J. M. Cook, K. E. G. Richter, C. E. Nolan, J. B. Schachter, F. Janat, Y. Che, V. Shanmugasundaram, B. A. Lefker, B. E. Enerson, E. Livni, L. Wang, N. J. Guehl, D. Patnaik, F. F. Wagner, R. Perlis, E. B. Holson, S. J. Haggarty, G. El Fakhri, R. G. Kurumbail,* N. Vasdev* **9601 – 9605**

Discovery of a Highly Selective Glycogen Synthase Kinase-3 Inhibitor (PF-04802367) That Modulates Tau Phosphorylation in the Brain: Translation for PET Neuroimaging

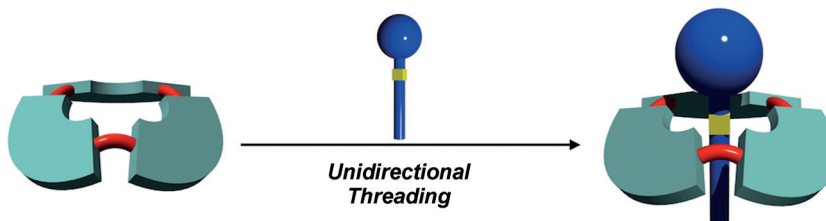


Molecular Recognition

T. Nakamura, G. Yamaguchi,
T. Nabeshima* 9606–9609



Unidirectional Threading into a Bowl-Shaped Macrocyclic Trimer of Boron–Dipyrin Complexes through Multipoint Recognition



Going in to bowl: A bowl-shaped macrocyclic trimer of a boron–dipyrin complex has been synthesized in which six polarized B–F bonds are directed towards the center of the macrocycle for strong recognition. Cationic ammonium guests are

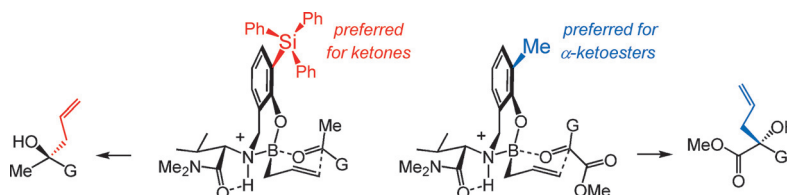
strongly captured from the convex side of the macrocycle by hydrogen bonding, Coulomb forces, and C–H... π interactions and thread unidirectionally through the complex.

Enantioselective Synthesis

D. W. Robbins, K. Lee, D. L. Silverio,
A. Volkov, S. Torker,
A. H. Hoveyda* 9610–9614



Practical and Broadly Applicable Catalytic Enantioselective Additions of Allyl-B(pin) Compounds to Ketones and α -Ketoesters



Easy to tune: A set of broadly applicable methods for efficient catalytic additions of easy-to-handle allyl-B(pin) (pin = pinacolato) compounds to ketones and acyclic α -ketoesters is introduced. Accordingly, a large array of tertiary alcohols can be

obtained in up to around 98 % yield and 99:1 e.r. Mechanism-based modification of the structures of aminophenol-based catalysts results in substantial improvement in enantioselectivity.

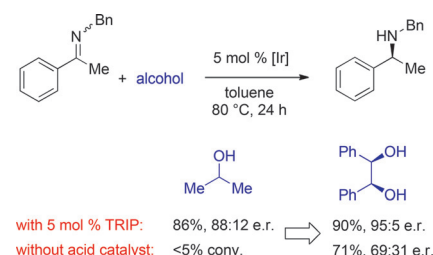
Reduction

H.-J. Pan, Y. Zhang, C. Shan, Z. Yu, Y. Lan,*
Y. Zhao* 9615–9619



Asymmetric Transfer Hydrogenation of Imines using Alcohol: Efficiency and Selectivity are Influenced by the Hydrogen Donor

The influence of alcohol, as the hydrogen donor, on the efficiency and enantioselectivity of the asymmetric transfer hydrogenation (ATH) of imines is reported. This discovery not only leads to a highly enantioselective access to *N*-aryl as well as *N*-alkyl chiral amines, but also provides new insight into the mechanism of iridium-catalyzed ATH of imines using alcohol.

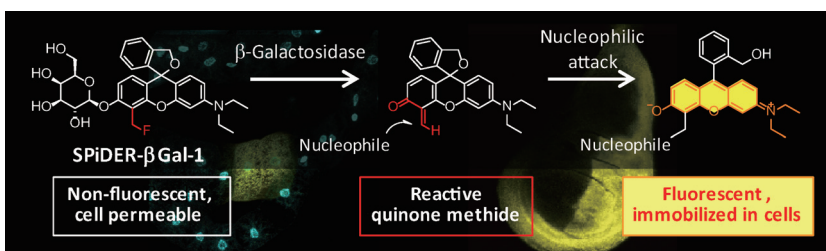


Fluorescent Probes

T. Doura, M. Kamiya,* F. Obata,
Y. Yamaguchi, T. Y. Hiyama, T. Matsuda,
A. Fukamizu, M. Noda, M. Miura,
Y. Urano* 9620–9624



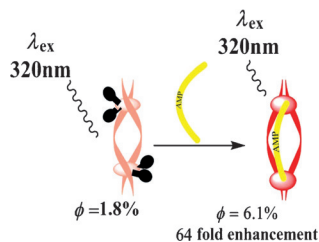
Detection of *LacZ*-Positive Cells in Living Tissue with Single-Cell Resolution



To detect *lacZ*-positive cells in living organisms or tissues at single-cell resolution, a fluorogenic β -galactosidase substrate, SPiDER- β Gal-1, was synthesized. The substrate exhibited a dramatic

increase in fluorescence upon reaction with the enzyme, remained inside cells by anchoring itself to intracellular proteins, and provided single-cell resolution.

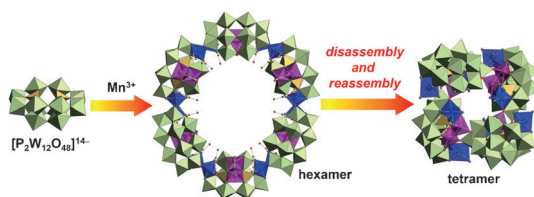
One AMP is enough: A coordinatively unsaturated double-stranded dinuclear europium(III) helicate shows adenosine monophosphate (AMP)-specific luminescence response even in the presence of highly charged adenosine di- or triphosphate (ADP or ATP).



Luminescence Sensors

J. Sahoo, R. Arunachalam, P. S. Subramanian,* E. Suresh, A. Valkonen, K. Rissanen, M. Albrecht* — 9625 – 9629

Coordinatively Unsaturated Lanthanide(III) Helicates: Luminescence Sensors for Adenosine Monophosphate in Aqueous Media



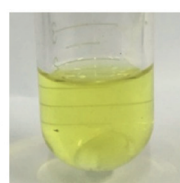
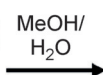
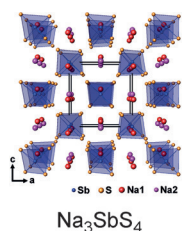
Giant rings: A manganese-substituted hexavacant lacunary Dawson-type phosphotungstate with two types of interaction sites undergoes disassembly and reas-

sembly without isomerization of the monomeric units. The inner cavity of the hexamer is the largest ever reported for a ring-shaped polyoxotungstate.

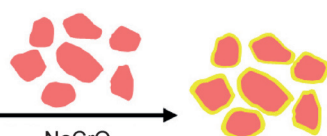
Polyoxometalates

T. Minato, K. Suzuki, K. Yamaguchi, N. Mizuno* — 9630 – 9633

Synthesis and Disassembly/Reassembly of Giant Ring-Shaped Polyoxotungstate Oligomers



Coating solution



Na₃SbS₄-coated NaCrO₂

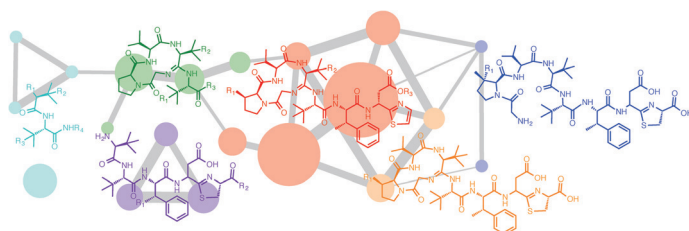
Dissolve and solidify: A new and highly conductive (1.1 mS cm⁻¹), dry air-stable sodium superionic conductor, tetragonal Na₃SbS₄, was developed. Importantly, its solution processability using methanol or water allows direct coating onto active

materials. The solution-processed highly conductive (0.1–0.3 mS cm⁻¹) solidified Na₃SbS₄ coating on NaCrO₂ solves the poor ionic contact problem in all-solid-state sodium-ion batteries.

Sodium-Ion Batteries

A. Banerjee, K. H. Park, J. W. Heo, Y. J. Nam, C. K. Moon, S. M. Oh, S.-T. Hong,* Y. S. Jung* — 9634 – 9638

Na₃SbS₄: A Solution Processable Sodium Superionic Conductor for All-Solid-State Sodium-Ion Batteries



A detailed understanding of bottromycin biosynthesis was obtained by harnessing a mass-spectral network (represented by colored nodes in the picture) to analyze a series of pathway mutants. This method

provides fresh insights into how this potent antibiotic is assembled, and shows that a YcaO domain protein works with a hydrolase-like protein to catalyze the formation of the macrocyclic amidine.

Biosynthesis

W. J. K. Crone, N. M. Vior, J. Santos-Aberturas, L. G. Schmitz, F. J. Leeper, A. W. Truman* — 9639 – 9643

Dissecting Bottromycin Biosynthesis Using Comparative Untargeted Metabolomics

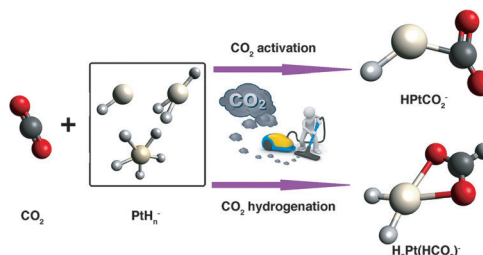


Metal Hydrides

X. Zhang, G. Liu, K. Meiwe-Broer,
G. Ganteför, K. Bowen* — 9644–9647



CO₂ Activation and Hydrogenation by
PtH_n[−] Cluster Anions



Metal hydride clusters: Naked (ligand-less) transition metal hydride cluster utilization in CO₂ activation and fixation was observed for the first time. A number of PtH_n[−] cluster anions were good hydro-

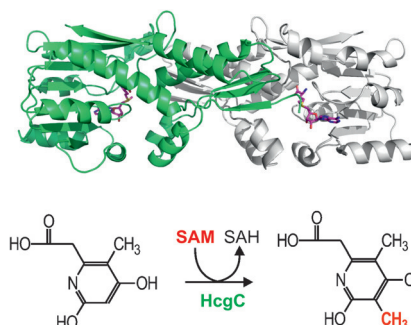
gen sources for the transformation of CO₂ into other higher value molecules, such as formate. Theoretical simulations validate the chemical reactions between the metal hydrides and CO₂.

Biosynthesis

T. Fujishiro, L. Bai, T. Xu, X. Xie, M. Schick,
J. Kahnt, M. Rother, X. Hu, U. Ermler,
S. Shima* — 9648–9651



Identification of HcgC as a SAM-
Dependent Pyridinol Methyltransferase in
[Fe]-Hydrogenase Cofactor Biosynthesis



Play it again, SAM: Biosynthesis of the iron guanylyl pyridinol cofactor of [Fe]-hydrogenase requires a challenging methyl transfer to the 3-position of the aromatic pyridinol ring. HcgC is predicted to be a novel S-adenosylmethionine (SAM)-dependent methyltransferase for catalyzing this reaction based on the crystal structures of HcgC with SAM and its demethylated product (SAH). The HcgC-catalyzed reaction was confirmed by enzymatic assays.

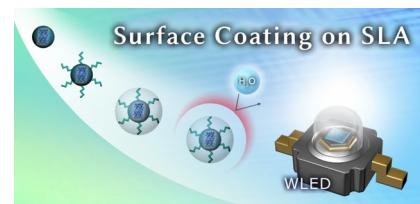
Light-Emitting Diodes

Y. T. Tsai, H.-D. Nguyen, A. Lazarowska,
S. Mahlik, M. Grinberg,
R. S. Liu* — 9652–9656



Improvement of the Water Resistance of
a Narrow-Band Red-Emitting
SrLiAl₃N₄:Eu²⁺ Phosphor Synthesized
under High Isostatic Pressure through
Coating with an Organosilica Layer

Stay dry and warm in this coat: The red-emitting phosphor SrLiAl₃N₄:Eu²⁺ has superior luminescence properties but is water-sensitive and generally synthesized from metal-hydride precursors. These limitations were overcome by the use of a high-pressure synthetic method and the application of an organosilica coating. The resulting material with enhanced optical properties was used to make high-performance warm-white-light-emitting diodes.

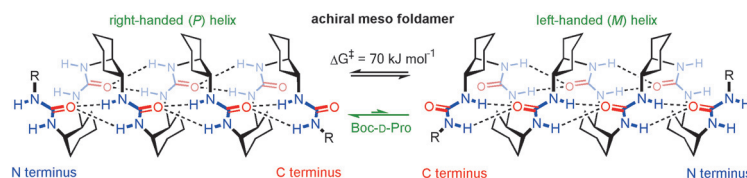


Conformational Analysis

R. Wechsel, J. Raftery, D. Cavagnat,
G. Guichard, J. Clayden* — 9657–9661



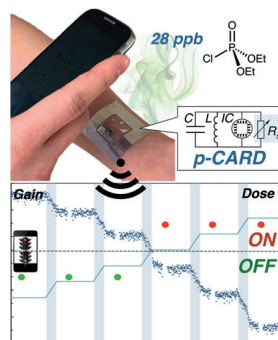
The *meso* Helix: Symmetry and Symmetry-
Breaking in Dynamic Oligoureia
Foldamers with Reversible Hydrogen-
Bond Polarity



Reversible foldamers: Urea oligomers of *meso*-cyclohexane-1,2-diamine form a dynamic racemic mixture of 2.5_{12/14} helices in which screw-sense inversion is

coupled with reversal of hydrogen-bond directionality. Desymmetrization induces a preferred directionality and screw sense.

Invisible dangers: A single-use, wirelessly addressable, highly sensitive, and selective chemical hazard badge that dosimetrically detects diethyl chlorophosphate, a nerve agent simulant, down to 28 ppb has been developed. The device comprises a wireless sensor platform and a chemidosimeter system incorporating single walled carbon nanotubes and ionic liquids. Exposure to 10 ppb DCP effects an irreversible switch in smartphone readout.



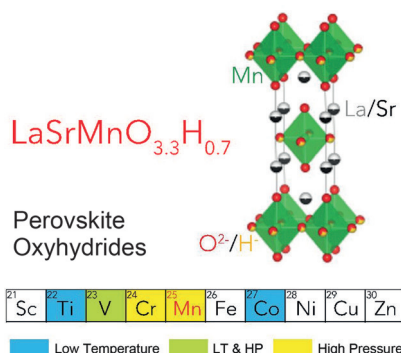
Sensors

R. Zhu, J. M. Azzarelli,
T. M. Swager* ————— 9662 – 9666

Wireless Hazard Badges to Detect Nerve-Agent Simulants



A high-pressure reaction provides access to a new manganese oxyhydride, $\text{LaSrMnO}_{3.3}\text{H}_{0.7}$, as opposed to topochemical reactions that yield only reduced oxides. $\text{LaSrMnO}_{3.3}\text{H}_{0.7}$ crystallizes in a single-layer perovskite structure, where H^- ions are selectively located at the equatorial site. It exhibits a spin glass transition at 22 K owing to competing ferro- and anti-ferromagnetic interactions.



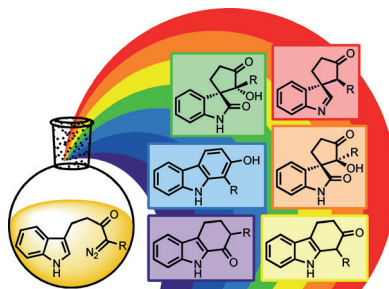
Solid-State Structures

C. Tassel, Y. Goto, D. Watabe, Y. Tang,
H. Lu, Y. Kuno, F. Takeiri, T. Yamamoto,
C. M. Brown, J. Hester, Y. Kobayashi,
H. Kageyama* ————— 9667 – 9670

High-Pressure Synthesis of Manganese Oxyhydride with Partial Anion Order



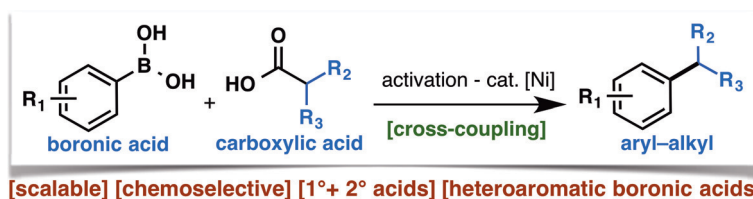
Pick a catalyst: Indolyl α -diazocarbonyls can be selectively cyclized to give six distinct products through the careful choice of the catalyst and reaction conditions. A range of catalysts were used, including complexes of Rh^{II} , Pd^{II} , and Cu^{II} as well as SiO_2 , to promote diazo decomposition and subsequent cyclization/rearrangement through a range of mechanistic pathways.



Diazo Compounds

M. J. James, P. O'Brien, R. J. K. Taylor,*
W. P. Unsworth* ————— 9671 – 9675

Selective Synthesis of Six Products from a Single Indolyl α -Diazocarbonyl Precursor



A cross-coupling between alkyl carboxylic acids and aryl boronic acids is enabled by a new activation/cross-coupling strategy under Nickel catalysis. The operational

simplicity and the wide range of heterocyclic compounds make a convenient strategy for obtaining aryl-alkyl cross-coupling products.

Cross-Coupling Reactions

J. Wang, T. Qin, T.-G. Chen, L. Wimmer,
J. T. Edwards, J. Cornella, B. Vokits,
S. A. Shaw, P. S. Baran* — 9676 – 9679

Nickel-Catalyzed Cross-Coupling of Redox-Active Esters with Boronic Acids



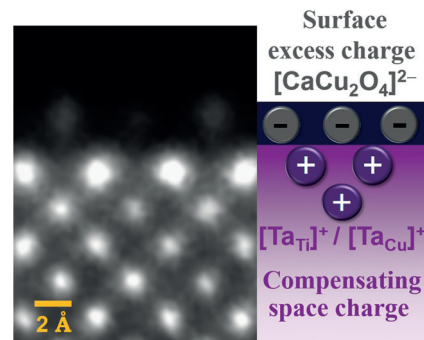
Perovskite Oxides

S.-Y. Chung,* S.-Y. Choi, H.-I. Yoon,
H.-S. Kim, H. B. Bae — 9680–9684



Subsurface Space-Charge Dopant Segregation to Compensate Surface Excess Charge in a Perovskite Oxide

Below the surface: Space-charge-driven dopant segregation in the subsurface region of an oxide, rather than the surface itself, is directly visualized with atomic resolution by transmission electron microscopy. A combination of atomic column resolved images and chemical analyses clarify the position of segregation.

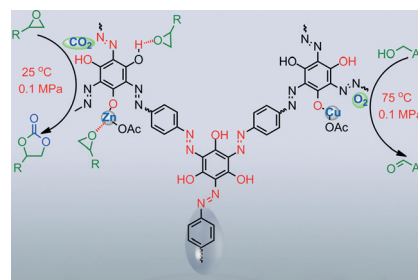
CO₂ Capture

G. P. Ji, Z. Yang, H. Zhang, Y. Zhao, B. Yu,
Z. Ma, Z. M. Liu* — 9685–9689



Hierarchically Mesoporous *o*-Hydroxyazobenzene Polymers: Synthesis and Their Applications in CO₂ Capture and Conversion

CO₂ just POPs in: In water and without any templates, hierarchically mesoporous *o*-hydroxyazobenzene polymers with high surface areas are synthesized. The porous organic polymers (POPs) showed excellent solubility in polar and apolar solvents, good adsorption capacity for metal ions, ultrahigh selectivity for CO₂/N₂ separation, and excellent performance for catalyzing CO₂ conversion.



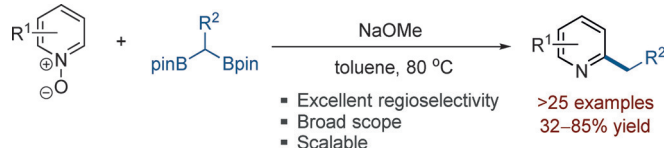
Back Cover

Heterocycles

W. Jo, J. Kim, S. Choi,
S. H. Cho* — 9690–9694



Transition-Metal-Free Regioselective Alkylation of Pyridine *N*-Oxides Using 1,1-Diborylalkanes as Alkylating Reagents



Going to the source: The transition-metal-free alkylation of pyridine *N*-oxides using 1,1-diborylalkanes as alkyl sources proceeds efficiently for a wide range of

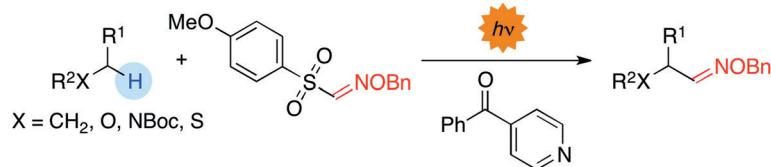
pyridine *N*-oxides and 1,1-diborylalkanes with excellent regioselectivity, thus affording C2-alkylated pyridines in good yields.

C–H Bond Formylation

S. Kamijo,* G. Takao, K. Kamijo,
M. Hirota, K. Tao,
T. Murafuji — 9695–9699

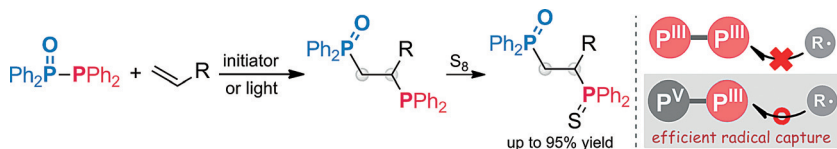


Photo-induced Substitutive Introduction of the Aldoxime Functional Group to Carbon Chains: A Formal Formylation of Non-Acidic C(sp³)–H Bonds



Formally formyl: A photo-induced substitutive introduction of an aldoxime functional group to carbon chains was achieved using photo-excited 4-benzoylpyridine and arylsulfonyl oxime. This is

a newly developed method for formal formylation of non-acidic C(sp³)–H bonds in a single step that proceeds at room temperature under neutral conditions.



P(O)P by: $\text{Ph}_2\text{P}(\text{O})\text{PPh}_2$ can engage in radical addition to various alkenes, thus affording the corresponding 1-phosphinyl-2-phosphinoalkanes regioselectively, and they can be converted into their sulfides by treatment with S_8 . The reaction pro-

ceeds by homolytic cleavage of the $\text{P}^{\text{V}}(\text{O})-\text{P}^{\text{III}}$ bond of $\text{Ph}_2\text{P}(\text{O})\text{PPh}_2$, selective attack of the phosphinyl radical at the terminal position of the alkene, and selective trapping of the resulting carbon radical by the phosphino group.

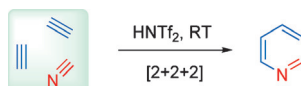
Phosphanes

Y. Sato, S.-i. Kawaguchi,* A. Nomoto, A. Ogawa* — 9700–9703

Highly Selective
Phosphinylphosphination of Alkenes with
Tetraphenyldiphosphine Monoxide



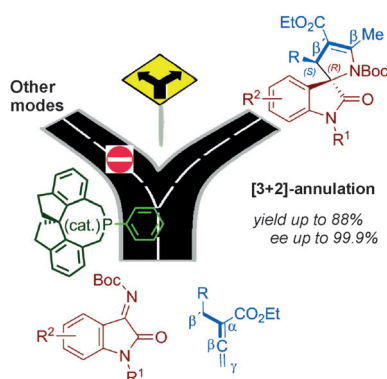
Triple two: A metal-free [2+2+2] cycloaddition of internal ynamides and nitriles was developed for the de novo synthesis of fully substituted pyridines. In contrast to metal catalysis, the versatile Brønsted acid HNTf_2 smoothly catalyzes the mild intermolecular cyclotrimerization of a range of ynamides and unactivated nitriles with complementary chemoselectivity.



Cyclotrimerization

Y. Wang, L.-J. Song, X. Zhang,* J. Sun* — 9704–9708

Metal-Free [2+2+2] Cycloaddition of
Ynamides and Nitriles: Mild and
Regioselective Synthesis of Fully
Substituted Pyridines

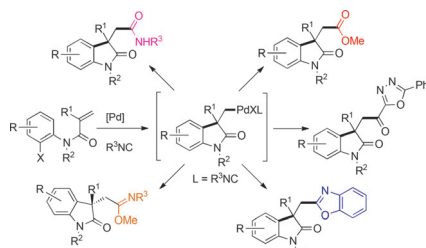


Taming a zwitterion: Chiral phosphine (*R*)- or (*S*)-SITCP generates a zwitterion from α -substituted allene ester that can engage the isatine derived ketimines in an unprecedented mode of [3+2] annulation reaction. This provides a facile asymmetric access to 3,2'-pyrrolidinyl spirooxindoles.

Asymmetric Phosphine Catalysis

M. G. Sankar, M. Garcia-Castro, C. Golz, C. Strohmann, K. Kumar* — 9709–9713

Engaging Allene-Derived Zwitterions in an
Unprecedented Mode of Asymmetric
[3+2]-Annulation Reaction



Setting a trap: The palladium-catalyzed reaction of *N*-aryl acrylamides with isocyanides affords diversely functionalized 3,3-disubstituted oxindoles by carbopalladation, migratory insertion of isocyanide, and nucleophilic trapping of the resulting alkylimido- Pd^{II} complex. An enantioselective protocol has also been developed using 2,6-diisopropylphenyl isocyanide as a reaction partner and a chiral ligand.

Heterocycles

W. Kong, Q. Wang, J. Zhu* — 9714–9718

Synthesis of Diversely Functionalized
Oxindoles Enabled by Migratory Insertion
of Isocyanide to a Transient
 σ -Alkylpalladium(II) Complex



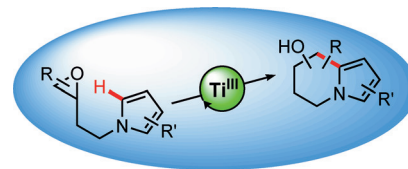
Catalysis

S. Hildebrandt,
A. Gansäuer* 9719–9722



Synthesis of Dihydropyrrolizine and Tetrahydroindolizine Scaffolds from Pyrroles by Titanocene(III) Catalysis

Bicycles Ti-cycles: The catalytic formation of dihydropyrrolizines and tetrahydroindolizines through titanocene(III) catalysis is described. The radical reaction is atom-economical, tolerates a large variety of functional groups, and proceeds with regioselectivity. It is therefore of interest for applications in the synthesis of biologically active compounds.



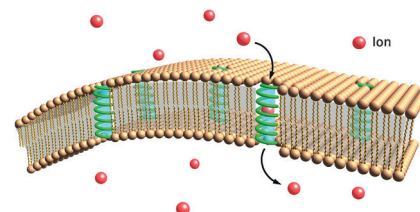
Helical Macromolecules

C. Lang, W. F. Li, Z. Y. Dong,* X. Zhang,
F. H. Yang, B. Yang, X. L. Deng,
C. Y. Zhang, J. Y. Xu,
J. Q. Liu* 9723–9727



Biomimetic Transmembrane Channels with High Stability and Transporting Efficiency from Helically Folded Macromolecules

Opening the door: An artificial unimolecular transmembrane channel using pore-containing helical macromolecules is presented. The self-folding, shape-persistent helical macromolecules span the lipid bilayer, resulting in extraordinary channel stability and high transporting efficiency for protons and cations. The lifetime of this channel in the lipid bilayer membrane is impressively long, rivaling those of natural protein channels.

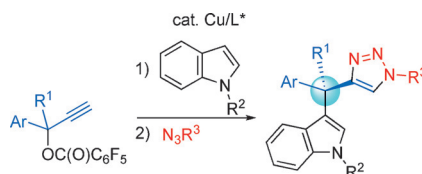


Enantioselectivity

K. Tsuchida, Y. Senda, K. Nakajima,
Y. Nishibayashi* 9728–9732



Construction of Chiral Tri- and Tetra-Arylmethanes Bearing Quaternary Carbon Centers: Copper-Catalyzed Enantioselective Propargylation of Indoles with Propargylic Esters



All-star all-carbon: The title reaction leads to the enantioselective construction of an all-carbon quaternary stereocenter. The subsequent derivatization of terminal alkyne moiety, into aromatic rings, is useful for the construction of chiral all-carbon substituted tri- and tetra-arylmethanes. The one-pot procedure demonstrated herein provides a successful example of the enantioselective preparation of a tetraarylmethane.

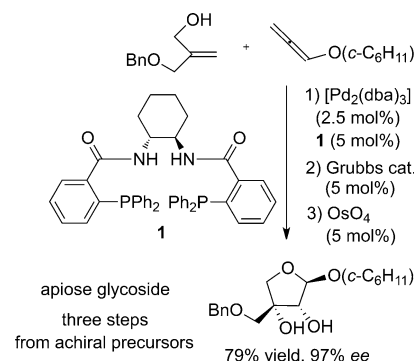
Carbohydrate Synthesis

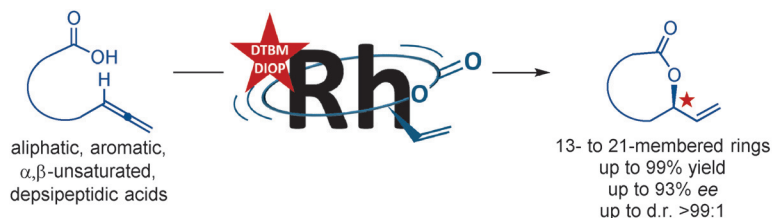
M. Kim, S. Kang,
Y. H. Rhee* 9733–9737



De Novo Synthesis of Furanose Sugars: Catalytic Asymmetric Synthesis of Apiose and Apiose-Containing Oligosaccharides

Special sugars call for special measures: In a concise synthetic approach to apiose, a structurally unusual furanose, the palladium-catalyzed asymmetric intermolecular hydroalkoxylation of an alkoxyallene was followed by ring-closing metathesis and dihydroxylation (see scheme). This strategy enabled the efficient synthesis of various apiose-containing disaccharides and was used in a unique convergent synthesis of trisaccharides.





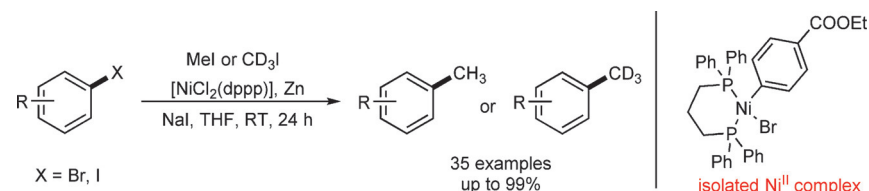
Reaching for stars: An intramolecular rhodium-catalyzed hydroxycarbonylation of ω -allenyl-substituted carboxylic acids in the presence of a chiral phosphine ligand

permitted the direct asymmetric formation of macrolactones (see scheme). The macrolactonization proceeded with good to high enantio- and diastereoselectivity.

Asymmetric Catalysis

S. Ganss, B. Breit* — 9738–9742

Enantioselective Rhodium-Catalyzed Atom-Economical Macrolactonization



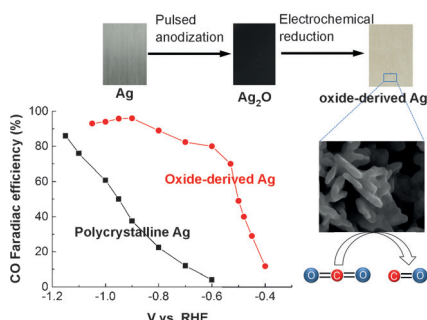
Introducing CD₃: A nickel-catalyzed reaction suitable for the cross-coupling of aryl halides with cheap and readily available CH₃I or CD₃I is reported. The reaction is applicable to a wide range of substrates and produces the desired product in

typically excellent yield. In particular, the reaction allows installation of a CD₃ group under the mild reaction conditions, without deuterium scrambling to other carbon atoms.

Cross-Coupling

L. Hu, X. Liu, X. Liao* — 9743–9747

Nickel-Catalyzed Methylation of Aryl Halides with Deuterated Methyl Iodide

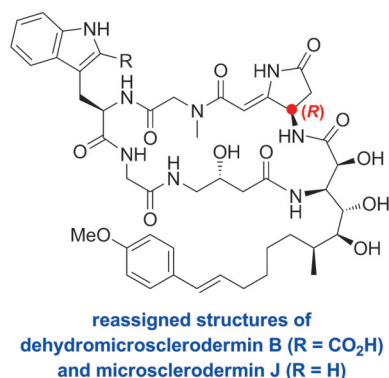


Nanostructured surfaces: An oxide-derived silver electrocatalyst was synthesized for the conversion of carbon dioxide to carbon monoxide with a high Faraday efficiency at low overpotentials. The nanostructure of the catalyst lowered the overpotentials as compared to polycrystalline silver by creating a high local pH value near the surface of the catalyst.

Electrocatalysis

M. Ma, B. J. Trzeźniewski, J. Xie, W. A. Smith* — 9748–9752

Selective and Efficient Reduction of Carbon Dioxide to Carbon Monoxide on Oxide-Derived Nanostructured Silver Electrocatalysts



Not your everyday AAs: Efficient approaches to the unusual amino acids in the title compounds were developed on the basis of the Negishi coupling (for the Trp-2-CO₂H) and the Blaise reaction (for the pyrrolidinone unit). The original assignment of the pyrrolidinone stereostructure was confirmed to be incorrect by the synthesis of epimers, whose spectroscopic data were in complete agreement with those for the natural isolates (see structure).

Cyclic Hexapeptides

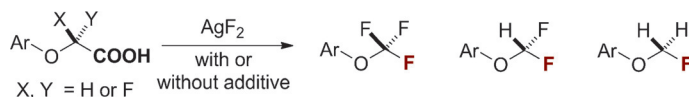
E. Y. Melikhova, R. D. C. Pullin, C. Winter, T. J. Donohoe* — 9753–9757

Dehydromicrosclerodermin B and Microsclerodermin J: Total Synthesis and Structural Revision



Fluorination

Q.-W. Zhang, A. T. Brusoe, V. Mascitti,
K. D. Hesp, D. C. Blakemore, J. T. Kohrt,
J. F. Hartwig* ————— 9758–9762



Radical F: AgF_2 induces fluorodecarboxylation of phenoxy difluoroacetic acids to afford trifluoromethyl aryl ethers. Pyridine

additives modulate the reactivity of AgF_2 , and enable the reaction to proceed with a variety of substrates.

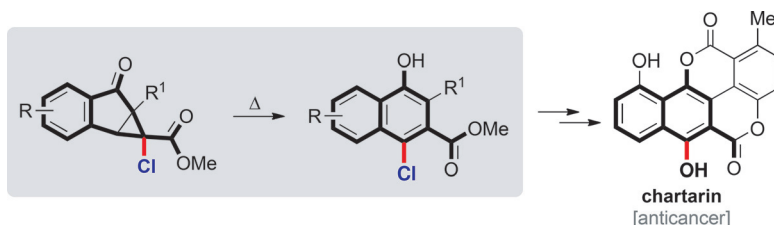


Fluorodecarboxylation for the Synthesis of Trifluoromethyl Aryl Ethers



Total Synthesis

T. A. Unzner, A. S. Grossmann,
T. Magauer* ————— 9763–9767



Substituted naphthalenes: Orthogonally functionalized naphthalenes were synthesized from commercially available indanones in four steps. The developed method proceeds through the thermally

induced fragmentation of cyclopropane indanones and involves a regioselective 1,2-chloride shift. This transformation enables the synthesis of the anticancer agent chartarin.



Rapid Access to Orthogonally Functionalized Naphthalenes: Application to the Total Synthesis of the Anticancer Agent Chartarin

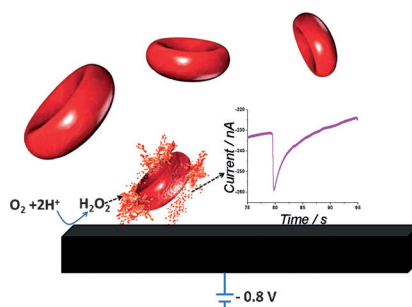


Electrochemistry

L. Sepunaru, S. V. Sokolov, J. Holter,
N. P. Young,
R. G. Compton* ————— 9768–9771



Electrochemical Red Blood Cell Counting: One at a Time



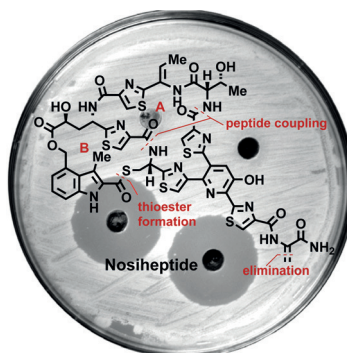
Catalytically active red blood cells: With the use of a nano-electrochemical technique fast and accurate red blood cell counting can be achieved together with complementary informations regarding the cell activity from each single cell. The method relies on the catalytic activity of red blood cells towards hydrogen peroxide and on surface-induced haemolysis.

Natural Product Synthesis

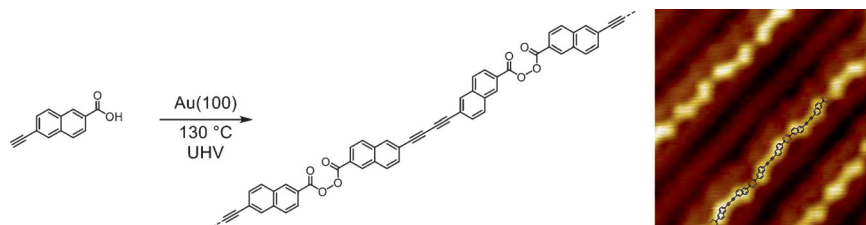
K. P. Wojtas, M. Riedrich, J.-Y. Lu,
P. Winter, T. Winkler, S. Walter,
H.-D. Arndt* ————— 9772–9776



Total Synthesis of Nosiheptide



Each ring is different: A total synthesis of the bismacrocyclic thiopetide antibiotic nosiheptide was achieved through the assembly of a fully functionalized linear precursor, followed by consecutive macrocyclizations. Key to success were the late-stage formation of a dehydroalanine residue and finely tuned deprotection of the hydroxypyridine core. The synthesis product was identical to the natural material in terms of structure and function.



Playing dominos on gold: 6-Ethynyl-2-naphthoic acid (ENA) undergoes on-surface Glaser coupling on gold to form 6,6'-(1,4-buta-1,3-diynyl)bis(2-naphthoic acid) (BDNA) which in turn reacts in an unprecedented dehydrogenative coupling

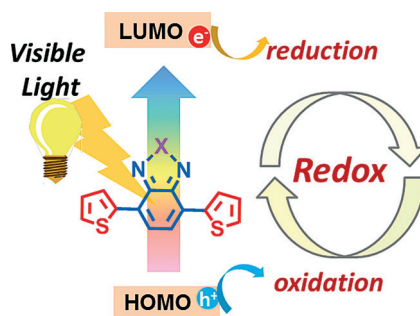
of the acid functionalities to give poly-BDNA. Polymeric chains with a length of over 100 nm can be obtained and the reaction outcome is influenced by the Au-surface topography and the surface coverage.

Surface Reactions

P. A. Held, H.-Y. Gao,* L. Liu, C. Mück-Lichtenfeld, A. Timmer, H. Mönig, D. Barton, J. Neugebauer, H. Fuchs,* A. Studer* — 9777–9782

On-Surface Domino Reactions: Glaser Coupling and Dehydrogenative Coupling of a Biscarboxylic Acid To Form Polymeric Bisacylperoxides

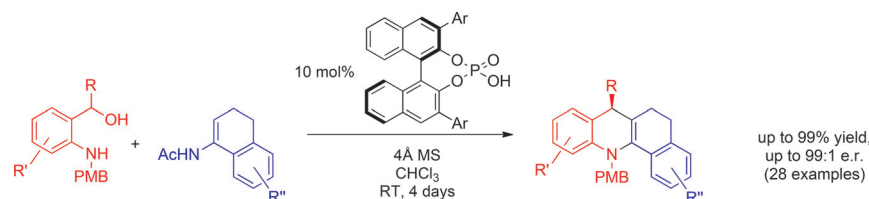
Give and take: Small-molecule organic semiconductor donor–acceptor systems with a tunable absorption range and defined energy-band structure are designed as metal-free, pure organic, visible-light-active photocatalysts to meet crucial requirements, such as absorption in the visible region, sufficient light-generated redox potential, and long exciton lifetime.



Photoredox Catalysis

L. Wang, W. Huang, R. Li, D. Gehrig, P. W. M. Blom, K. Landfester, K. A. I. Zhang* — 9783–9787

Structural Design Principle of Small-Molecule Organic Semiconductors for Metal-Free, Visible-Light-Promoted Photocatalysis



Complex N-heterocycles in one shot: *ortho*-Quinone methide imines generated in situ react with enamides with high enantioselectivity under phosphoric acid catalysis giving valuable chiral tetrahydroacridines in one step. Subsequent diastereoselective hydrogenation provides saturated N-heterocycles with a total of three new stereocenters. PMB = *p*-methoxybenzyl.

droacridines in one step. Subsequent diastereoselective hydrogenation provides saturated N-heterocycles with a total of three new stereocenters. PMB = *p*-methoxybenzyl.

Organocatalysis

M. Kretschmar, T. Hodík, C. Schneider* — 9788–9792

Brønsted Acid Catalyzed Addition of Enamides to *ortho*-Quinone Methide Imines—An Efficient and Highly Enantioselective Synthesis of Chiral Tetrahydroacridines



Supporting information is available on www.angewandte.org (see article for access details).



A video clip is available as Supporting Information on www.angewandte.org (see article for access details).



This article is available online free of charge (Open Access).



This article is accompanied by a cover picture (front or back cover, and inside or outside).



The Very Important Papers, marked VIP, have been rated unanimously as very important by the referees.



The Hot Papers are articles that the Editors have chosen on the basis of the referee reports to be of particular importance for an intensely studied area of research.